Synthesis of Bulk MgB_2 Superconductors by Pulsed Electric Current

A. M. Locci, R. Orrù and G. Cao
Dipartimento di Ingegneria Chimica e Materiali, Unità di Ricerca del Consorzio Interuniversitario per la Scienza e Tecnologia dei Materiali (INSTM), Università degli Studi di Cagliari, Piazza d'Armi, 09123 Cagliari, Italy and PROMEA Scarl, c/o Dipartimento di Fisica, Cittadella Universitaria di Monserrato, S.S. 554 bivio per Sestu, 09042 Monserrato (CA), Italy

S. Sanna, F. Congiu, and G. Concas
Dipartimento di Fisica, Università degli Studi di Cagliari and CNISM, S.P. Monserrato-Sestu km 0.700, I-09042 Monserrato (CA), Italy

DOI 10.1002/aic.10846
Published online April 21, 2006 in Wiley InterScience (www.interscience.wiley.com).

A preparation method to simultaneously synthesize and consolidate bulk MgB_2 superconductors from Mg and B commercial elemental powders by means of the spark plasma sintering technique is reported. The influence of process parameters on sintering process dynamics as well as product characteristics, determined by transport and magnetic measurements, is investigated. The superconducting properties of the obtained samples, and particularly the critical current density, are comparable or better than those corresponding to other MgB_2 preparation techniques. Thus, the superconductive properties of the bulk MgB_2 materials synthesized in this work are suitable for selected applications, such as magnetic levitation, magnetic screening, and fault current limiters. It should be finally noted that the proposed method represents a particularly rapid preparation route as compared to other techniques. © 2006 American Institute of Chemical Engineers *AIChE J,* 52: 2618–2626, 2006

Keywords: synthesis, densification, spark plasma, sintering, magnesium diboride, superconductivity

Introduction

The binary compound MgB_2, which has been known since the early 1950s of the last century,[1] was recently found to possess superconductive behavior at 39 K[2]. This transition temperature, T_C, is the highest one without considering fullerides and high-T_C cuprates superconductors. It is also significantly higher than that of Nb_3Ge, $T_C = 23.2$ K, which was previously reported as the highest T_C value for intermetallic compounds following the Bardeen-Cooper-Schrieffer (BCS) superconductivity theory. Therefore, since the recent discovery of MgB_2 superconductivity, its properties, synthesis routes, and possible applications have been extensively investigated.[3-5]

It is worth noting that the binary compound MgB_2 has become a strong candidate for superconductivity applications[6] because of its advantages with respect to all practical superconductors ($Nb_{47}Ti_{53}$, Nb_3Sn, YBCO, and Bi-2223). As compared to oxide superconductors, MgB_2 shows a simpler structure and it is expected to be less anisotropic than layered high temperature superconductors, thus minimizing grain boundaries' effect on superconducting properties. Moreover, due to its metallic nature, MgB_2 has lower normal state resistivity and it is characterized by lower cost production and easier metalworking.[6] With respect to intermetallic superconductors, the higher transition temperature represents the major advantage of MgB_2.[7]

Consequently, fabrication techniques to obtain MgB_2 sam-

Correspondence concerning this article should be addressed to G. Cao at cao@visnu.dicm.unica.it.

Table 1. Characteristics of the Starting Powders Used in the Present Investigation

Reactant	Vendor	Particle Size	Purity
Magnesium (Mg)	Alfa Aesar (10233)	−325 mesh	99.8%
Boron (B), crystalline	Sigma-Aldrich (21,472-8)	−325 mesh	90–95%
Boron (B), amorphous	Fluka (15580)	—	95–97%

ples in the forms of film, tape, wire, and bulk have been actively investigated. In particular, bulk magnesium diboride may be potentially employed for superconducting applications, besides the advantages mentioned above, because of its low mass density. This aspect would allow fabrication of desirable shapes, such as blocks, cylinders, and rods, with superconducting properties and open the way to applications like magnetic screening devices, inductive fault current limiters, magnetic bearings, and high power permanent magnets operating at intermediate temperatures between helium and nitrogen boiling points.[6]

The two main routes to prepare bulk MgB_2 are based on the reaction of pure elements (in situ technique) or the sintering of MgB_2 commercial powders (ex situ technique). In the first class of preparative methods, the elements are led to temperature typically above the melting point of magnesium (648°C) while in the ex situ methods, MgB_2 commercial powders are processed at temperatures in the range 900-1200°C. In particular, MgB_2 bulk specimens were usually prepared by heating the starting powders in vacuum or Ar atmosphere inside sealed Mo or Ta containers.[8,9] However, due to the high volatility of Mg at elevated temperatures, the bulk MgB_2-based superconductors produced by these methods show poor mechanical properties, weak grain connectivity, and high porosity.

Thus, processing methods to achieve fully dense MgB_2 bulk specimens have been sought for various purposes. Until now, simultaneous synthesis from pure elements and consolidation or sintering of MgB_2 commercial powders under extremely high isostatic pressures as high as several GPa[10,11] or hot uniaxial pressing in the range 30-100 MPa[12,13] have been effective to obtain MgB_2 bulk specimens. In addition, various other methods, such as liquid Mg infiltration of boron preforms,[14] microwave synthesis,[15] or shock wave consolidation of pre-alloyed powders,[16] have been proposed to synthesize bulk MgB_2.

Based on the simultaneous application of a mechanical pressure and a pulsed electric current, the Spark Plasma Sintering (SPS) technique has been recently proposed to make fully dense and fine-grained ceramic materials.[17] In particular, an MgB_2 bulk superconductor has been recently sintered by means of SPS starting from commercial MgB_2 powders.[18,19] This superconductor material has also been prepared using the same SPS technique starting from amorphous boron powders and MgH_2, which was, on the other hand, previously obtained through distillation in vacuum at 870 K of Mg pieces and subsequent hydrogenation under a pressure of 3 bar and a temperature of 600 K.[20]

In the present study, we report on a recently patented[21,22] route for the one step preparation of dense magnesium diboride starting from commercial powders of magnesium and boron by taking advantage of the spark plasma sintering technique. The influence of process parameters, that is, type of boron, synthesis time, temperature, and mechanical pressure conditions, on the SPS process dynamics as well as product characteristics is first investigated in this work. A comparison of the superconducting properties of the synthesized materials with respect to those prepared using the other techniques mentioned above is also reported. This systematic study has great importance since it has been found that physical properties for samples made under different process conditions are significantly different.[23] Therefore, for large scale applications, as well as for small scale electronic device applications, a clear relation between synthesis conditions and superconducting properties is highly desirable.

Experimental Section

The characteristics of the starting powders used in the present investigation as well as their sources are reported in Table 1. Magnesium and boron powders were weighted in the atomic ratio 1:2 and dry mixed in a SPEX 8000 mill for 30 min. Milling was done in a stainless steel jar using alumina balls.

An SPS 515S apparatus produced by Sumitomo Coal Mining Co. Ltd., Japan, was used to synthesize dense MgB_2. A schematic representation of the machine with details of the experimental set-up are shown in Figure 1. It combines a 50 kN uniaxial press with a DC pulsed current generator (10 V, 1500 A, 300 Hz) to simultaneously provide a pulsed electric current through the sample and the graphite die containing it, together with a mechanical load through the die plungers. Two cylindrical graphite blocks (diameter, 80 mm and 30 mm; and both height, 40 mm) were placed between the upper plunger and the upper electrode, as well as the lower plunger and the lower electrode. Die, plungers, and blocks were all made of AT101 graphite (Atal s.r.l., Italy).

About 1.5 g of powder mixture was first cold-compacted

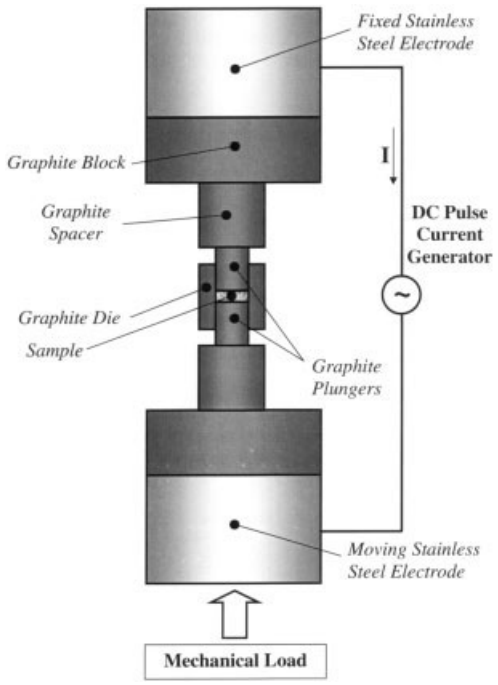

Figure 1. SPS apparatus.

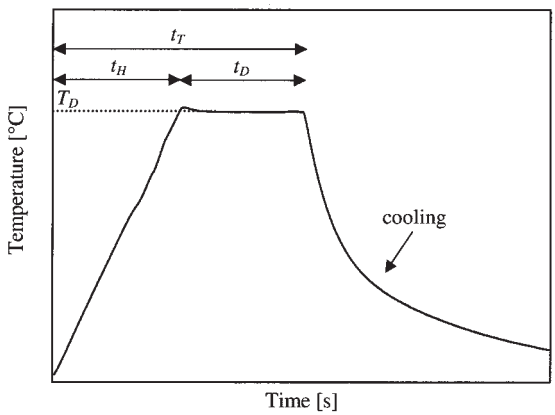

Figure 2. Temperature cycle adopted during SPS.

inside the die (outside diameter, 30 mm; inside diameter, 15 mm; height, 30 mm). In order to protect the die and facilitate the sample release after synthesis, a 99.8% pure graphite foil (0.13 mm thick, Alfa Aesar, Germany) was inserted between the internal surface of the die and between the top and the bottom surface of the sample and the graphite plungers (14.7 mm diameter, 20 mm height). The die was then placed inside the reaction chamber of the SPS apparatus and the system was evacuated down to 10 Pa. This step was followed by the application of mechanical pressure through the plungers.

The experiment is initiated with the application of a previously set temperature cycle schematically depicted in Figure 2, where T_D is the dwell temperature while t_D, t_H, and t_T represent the dwell, heating, and total times, respectively. Temperatures were measured during synthesis by a C-type thermocouple (OMEGA Engineering, Inc., USA), which was inserted inside a small hole in one side of the graphite die. Temperature, applied current, voltage, mechanical load, and vertical displacement (δ) of the lower electrode were measured in real time and recorded. The parameter δ can be regarded as the degree of compact densification. In fact, as a consequence of sample shrinkage, the lower electrode moves up because of the applied mechanical load. However, sample thermal expansion as well as that of both electrodes, graphite blocks, spacers, and plungers, contribute to vertical displacement changes. Therefore, the real degree of consolidation can be evaluated only by measuring sample density at the end of the process. For the sake of reproducibility, each experiment was repeated at least twice.

After the synthesis process, the sample was first allowed to naturally cool for about 30 min and was then removed from the die. The relative density of the product was determined by geometrical measurements and by the Archimedes method. Phase identification was performed on the obtained product once reduced in powder form by using a Philips PW 1830 X-rays diffractometer with Cu Kα radiation (λ = 1.5405 Å) and Ni filter. The 2θ range investigated was 20-70°, while scan time and scan step were 0.02 s and 0.01 deg, respectively. Microstructure of end products was examined by scanning electron microscopy (SEM) Hitachi S4000, and local phase composition was determined by energy dispersive X-ray spectroscopy (EDXS).

A SQUID magnetometer (mod. MPMS5 XL5, Quantum Design, San Diego, CA) was used to investigate the low-field DC magnetization of the samples both in powder and bulk form as a function of temperature with an applied magnetic field of 1 Oe. Magnetization versus magnetic field was measured at temperatures of 5 and 20 K; fields up to 50 kOe were used to determine the critical current density. The size of powder particles used for magnetization measurements has been examined by SEM. For resistivity evaluation, the SPS sample was cut by using a diamond saw (Secotom 10, Struers, Denmark) into rectangular solid shape with dimensions of about 4.7 $\times$ 1.6 $\times$ 14 mm^3. The resistivity curve, $R(T)$, was measured by an AC 4-probe technique using a current density of 4×10^{-4} A/mm^2 and a frequency of 33 Hz; the samples were cooled in a closed-cycle cryocooler.

Results and Discussion

Effect of boron powder characteristics

The influence of the type of boron powders, that is, amorphous or crystalline, employed in the starting mixture on the synthesis process of MgB_2 by SPS was investigated first. The dwell temperature, T_D, was in both cases set to 800°C while the heating time, t_H, and the total sintering/reaction time, t_T, were 5 and 10 min, respectively. The applied mechanical pressure was 50 MPa.

Let us first analyze the SPS outputs. When adopting the same temperature-time program conditions, current, voltage and shrinkage time profiles measured during the synthesis process were found similar, even though crystalline or amorphous boron were used. In particular, the profiles corresponding to the case of amorphous boron are reported in Figure 3, along with the prescribed time-temperature profile. It is seen that, as soon as the SPS experiment was started, in order to satisfy the thermal profile, the current gradually increases and so does the voltage (Figure 3a)). This behavior takes place until the temperature level reached by the die is below 550°C (Figure 3b)). No significant changes of the displacement δ are observed during the first 30 s. An almost linear increase (to about 0.25 mm) then takes place until δ undergoes a slight augment. The latter one is followed by a steep increase (to about 2.25 mm) in time, which corresponds to the temperature interval 550-650°C (Figure 3b)). The displacement then reaches an approximately constant value up to the interruption of the electric current application ($t = t_T$ = 10 min). The observed increase of δ when the application of the electric current is interrupted is a manifestation of the shrinkage of the sample ensemble (die/plungers/sample) due to thermal shrinkage accompanying system cooling. In particular, during the rapid sample displacement, the sample become denser and, therefore, the corresponding electrical resistance decreases. Thus, the current must increase more rapidly in order to follow the selected temperature-time profile. An analogous behavior is correspondingly observed for the voltage. Both current and voltage decrease when the stationary temperature value (800°C) is reached at 300 s. A further application of the current did not result in any appreciable variation of the displacement, while the observed increase of δ when the application of the electric current is interrupted (600 s) is a direct consequence of the die/plungers/sample thermal shrinkage that accompanies the cooling of the system.

Let us now consider the influence of the boron type used on

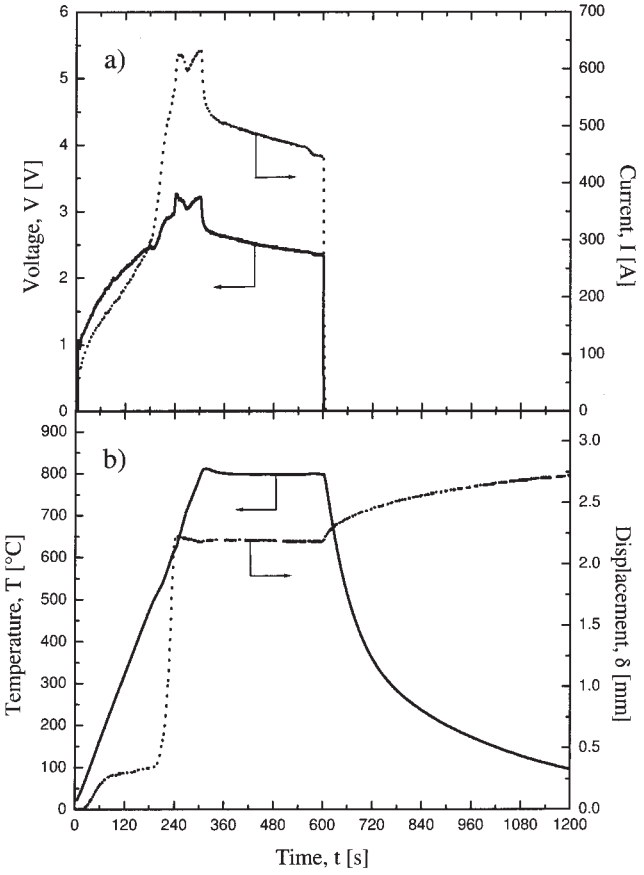

Figure 3. Temporal profiles of SPS outputs.

(a) Current intensity and voltage, (b) sample displacement and temperature (T_D = 800°C, P = 50 MPa, t_T = 10 min, t_D = 5 min).

the composition of the final product. Figures 4a and 4b show the XRD patterns of samples obtained using amorphous and crystalline boron powders, respectively. It is seen that, when amorphous boron powders were used, the conversion of the initial reactants to the desired phase MgB_2 is complete, as proven by the XRD pattern analysis of the SPS product, which reveals the presence of MgB_2 and only small amounts of MgO. Vice versa, when crystalline boron powders were utilized under the same SPS operating conditions, in addition to the desired phases of MgB_2, the product contained unreacted magnesium and boron, as well as a relatively larger amount of MgO.

The results above seem to indicate a higher reactivity of amorphous powders as compared to the crystalline ones. This aspect is consistent with the results reported in the literature, where the effect of the form (crystalline or amorphous) of boron was investigated for the synthesis of TiB_2-$TiAl_3$ composite by field-activated combustion.[24] In fact, it was found that, while the use of amorphous boron makes the synthesis reaction able to be self-sustained, this was not the case when crystalline boron was employed, where, on the other hand, an external energy source (electric field) was required to permit the propagation of the combustion synthesis reaction. On the basis of the results discussed above, the amorphous B powders were chosen for subsequent experiments.

Kinetic investigation of the synthesis process

The formation of MgB_2 during the SPS process has been subsequently monitored by simultaneously applying the pulsed electric current and mechanical pressure for different prefixed time intervals (t_T). Specifically, the influence of this parameter on the composition of the obtained SPS products was investigated under the experimental conditions considered in the previous paragraph, that is, temperature-time program as reported in Figure 3b and P = 50 MPa. The experiments have been performed by interrupting the application of the current at different times, which correspond particularly to the most significant changes in the displacement time profile (Figure 3b). The final samples obtained under these conditions have been analyzed by X-rays diffraction. The resulting patterns are reported in Figure 5, along with that corresponding to the starting powder mixture (Figure 5a). Since the boron was amorphous, it was not identified by this analysis. It is seen that the interruption of the current at about 210 s, that is, when the steep displacement starts to commence, shows that no significant interaction between the reactants takes place, as seen from the patterns of Figure 5b, which depicts peaks for Mg and small amounts of MgB_2 only. Conversely, as the reaction time is increased to about 240 s, that is, immediately after the end of the rapid variation of δ (Figure 3b), the desired end-phase is now present in the final product (Figure 5c). However, a complete conversion to the desired product is not yet achieved, as can be seen by the significant presence of magnesium peaks in the XRD pattern of the SPS sample. As the reaction time is increased to 360 s, the elemental reactants are almost totally converted to the diboride phase (Figure 5d). Finally, when the hold time in the SPS apparatus is prolonged to 600 s (Figure 5e), the desired product is obtained.

On the basis of the results described above, some considerations related to the displacement- and temperature-time profiles, and the corresponding physical and chemical transforma-

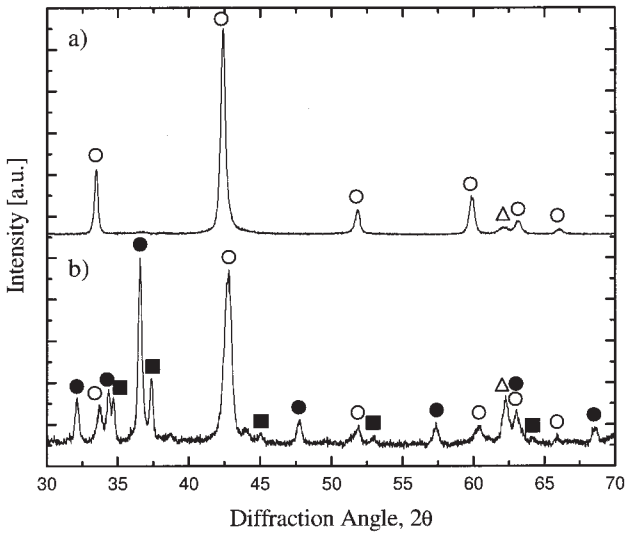

Figure 4. Effect of B powders on the composition of the final SPS product.

(a) Amorphous powders; (b) crystalline powders (T_D = 800°C, P = 50 MPa, t_T = 10 min, t_D = 5 min). [○MgB_2; △ MgO; ● Mg; ■ B].

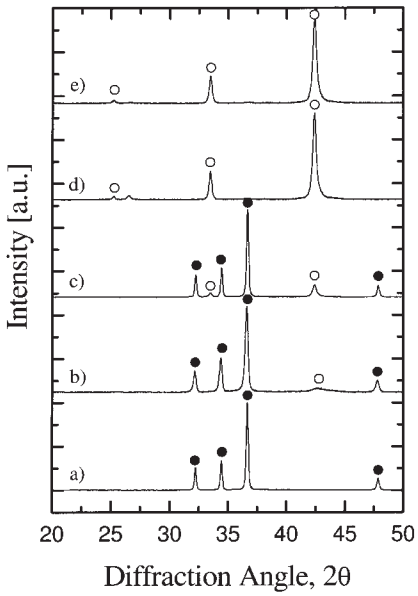

Figure 5. XRD patterns of SPS products obtained for different values of the time interval during which the pulsed electric current is applied.

(T_D = 800°C, P = 50 MPa). (a) Reactants; (b) t_T = 3.5 min; (c) t_T = 4 min; (d) t_T = 6 min; (e) t_T = 10 min. [○ MgB_2; ● Mg].

tion taking place during the synthesis and simultaneous consolidation of MgB_2 by SPS, can be made. It can be first concluded that below 550°C, during which time the sample shrinkage is relatively low, neither chemical nor physical significant transformation are observed to occur in the powder compact.

On the other hand, considerable shrinkage was observed to occur when the temperature level reached was in the range 550-650°C (Figure 3b). During this temperature interval, the melting of Mg (648°C) is expected to take place only at the end of the observed remarkable change of δ. However, it is worth noting that, as reported in the Experimental Section, temperature measurements were performed in the graphite die using a thermocouple inserted inside a small hole. Based on this, it is likely that the temperature in the reacting sample can locally reach higher values, as compared to those reported in Figure 3b, and, therefore, the rapid sample densification can be associated to the melting of Mg. At this point, Mg starts to react with B to form the diboride phase. This is in accordance with the recent results reported in the literature on this issue.[25-27] In particular, Yan et al.[27] investigated experimentally the MgB_2 synthesis process by differential thermal analysis (DTA). The obtained DTA curve clearly displays that the occurrence of the formation of the MgB_2 phase is preceded by Mg melting.

Effect of dwell temperature level

The effect of dwell temperature, T_D, on the synthesis of MgB_2 by means of the SPS process was subsequently studied by simultaneously applying a constant mechanical pressure (P = 50 MPa) and setting different T_D values, that is, 600, 700, 800, 900, and 1000°C. The heating time, t_H, and the dwell time, t_D, were both 5 min in order to maintain a total synthesis time, t_T, equal to 10 min.

The XRD patterns of the obtained products are shown in Figure 6. When T_D was set equal to 600°C, no significant interaction between reactants takes place, as seen from the patterns reported in Figure 6a, which shows peaks for Mg only apart from the evidence of incipient formation of the desired product, MgB_2. It is worth noting that since amorphous boron powders were used, boron peaks could not be detected by this analysis. As the dwell temperature was increased to 700°C, the desired end-phase, MgB_2, is now significantly present in the final product (Figure 6b). However, a complete conversion to the desired product is not yet achieved. As the temperature T_D was increased to 800°C, the complete conversion of the starting reactants was obtained, as proven by the absence of residual magnesium in the XRD pattern, now showing peaks for MgB_2 only (Figure 6c). With an increase in the dwell temperature to 900°C (Figure 5d), the XRD pattern of the final product does not display remarkable differences as compared to the previous case. Conversely, when T_D is augmented to 1000°C, the situation drastically changes (Figure 6e). In fact, significant amounts of Mg and MgB_4 were found in the corresponding SPS sample along with MgB_2, as a result of the decomposition of the latter. This phenomenon is typically encountered during synthesis or sintering processes of magnesium diboride[27-29] and is consistent with the results provided by the thermodynamic studies recently conducted on the Mg-B system.[30] In the latter, the strong dependence of the thermodynamic stability of MgB_2 on the pressure conditions, mainly because of the high Mg volatility, is discussed. It is reported that the temperature values at which the decomposition reaction:

$$MgB_2 \rightarrow 0.5MgB_4 + 0.5Mg$$

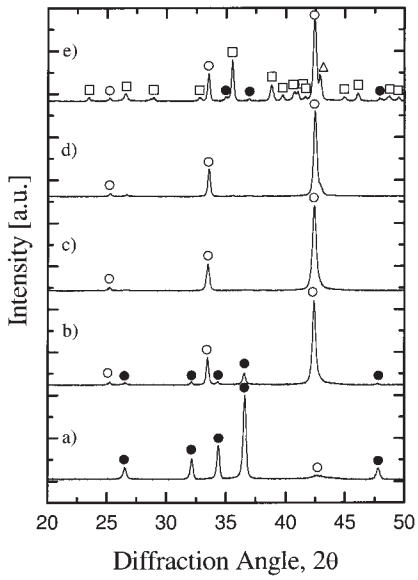

Figure 6. XRD patterns of SPS products obtained at different values of dwell temperature T_D.

(P = 50 MPa, t_T = 10 min, t_D = 5 min). (a) T_D = 600°C; (b) T_D = 700°C; (c) T_D = 800°C; (d) T_D = 900°C; (e) T_D = 1000°C. [○ MgB_2; △ MgO; □ MgB_4; ● Mg].

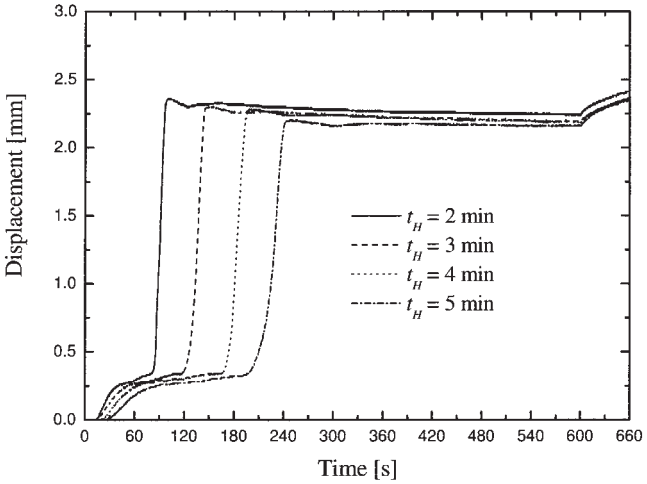

Figure 7. Temporal profiles of sample displacement obtained at different levels of heating rate (T_D = 800°C, P = 50 MPa, t_T = 10 min).

takes place are about 600, 950, or 1550°C under the pressures of 1 mTorr, 1 Torr, and 1 atm, respectively. Specifically, under the gas pressure conditions adopted in our work during the SPS process, that is, about 10^{-2} Torr, the decomposition of MgB_2 to form MgB_4 is then estimated to occur at about 900°C. This finding is in accordance with the results obtained in this work, although the presence of MgB_4 from XRD is revealed only at 1000°C (Figure 6e). In fact, its formation is not excluded even at 900°C, even if the amount of this phase is relatively low and, therefore, not detectable using this technique.

The results shown above seem to indicate that, in order to guarantee the interaction between magnesium and boron during the SPS process, the synthesis temperature should be higher than 600°C. In addition, the complete conversion of starting reactants to the desired phase MgB_2 can be obtained with temperature greater than 700°C but lower than 900°C in order to avoid its decomposition.

Effect of heating rate

The effect of heating rate on process dynamics was investigated by varying t_H (Figure 2) in the range 2-60 min. The obtained shrinkage displacement profiles measured during the synthesis process are shown in Figure 7 for selected different values of t_H, that is, 2, 3, 4, and 5 min, while keeping constant the total time, that is, t_T = 10 minutes. It is clearly seen that as the heating rate is augmented, the position of the curves where the steep sample displacement takes place is anticipated while its slope slightly increases. This fact means that, as the heating rate is increased, the melting of Mg and, consequently, the onset of the transformation of elemental reactants to the desired MgB_2 product, is anticipated. It is worth noting that this event occurs before the dwell temperature is reached, that is, during the heating step, regardless of the heating rate conditions.

Densification process

So far, the attention has been mainly focused on the reaction synthesis. However, since the objective of the work is also to obtain a bulk material, the consolidation process represents an important issue to be investigated. The evolution of densification phenomena during the synthesis of MgB_2 by SPS can be deduced from Table 2, where the end-products density has been reported as a function of the time intervals during which the current is applied. It is seen that, under the prescribed experimental condition, that is, the temperature-time program reported in Figure 3b, the most significant consolidation takes place during the time interval 3.5-4 min, according to the displacement-time profile also shown in Figure 3b. As the hold time is increased up to 6 min, the densification process proceeds but at a much lower rate. A further increase of t_T up to 20 min did not result in significant changes of sample density. Specifically, the maximum level of the end-product density reached under these conditions was about 76% of the theoretical value (2.63 g/cm^3).

Table 2. Densities of Products Obtained by SPS as a Function of the Time Interval During Which the Pulsed Electric Current is Applied [T_D = 800°C, t_H = 5 min, P = 50 MPa]

Sample ID	t_T [min]	ρ [g/cm^3]
A	3.5	1.55
B	4	1.83
C	6	1.99
D	10	1.93
E	20	1.91

The influence of the heating rate conditions on the relative density of the SPS products was then investigated and the obtained results, which are all characterized by the complete conversion of reactants into the desired product, are summarized in Table 3. From that Table, it is clearly seen that a variation of this parameter does not induce significant changes in the density of the product, with the latter one always in the range 73.4-77.3% of the MgB_2 theoretical value.

The influence of the mechanical load applied during the SPS process on the densification of MgB_2 was also studied. The mechanical pressure was varied in the range 50-100 MPa and the obtained results are reported in Table 4, for the case of T_D = 800°C, t_H = 5 min, and t_T = 10 min. It is observed that the increase of the applied load is accompanied by only a little change in sample density, which is maintained in the range 73.4-74.2% of the theoretical value.

The obtained results have been confirmed by products characterization performed using scanning electron microscopy. As an example, Figure 8 shows a SEM micrograph of the sample obtained under the following process conditions: P = 50 MPa, T_D = 800°C, t_H = 5 min, t_T = 10 min (sample D in Table 2). It is clearly seen that the examined sample is characterized by residual porosity.

Table 3. Densities of End-Products Obtained by SPS as a Function of the Heating Rate [T_D = 800°C, P = 50 MPa]

Sample ID	t_H [min]	t_D [min]	t_T [min]	ρ [%]
F	2	8	10	77.3
G	3	7	10	76.9
H	4	6	10	75.5
D	5	5	10	73.4
L	10	5	15	74.5
M	20	5	25	77.2
N	60	5	65	77.2

Table 4. Densities of End-Products Obtained by SPS as a Function of the Applied Mechanical Pressure [T_D = 800°C, t_H = 5 min, t_T = 10 min]

Sample ID	P [MPa]	ρ [%]
D	50	73.4
P	75	74.2
Q	100	74.1

On the basis of the results reported above, it is apparent that the densification of MgB_2 is not an easy task to deal with. This aspect may be explained on the basis of the extremely high volatility of magnesium at high temperature whose significant evaporation, under vacuum conditions, was found to start near 425°C.[31] For this reason, it is very difficult to prepare full dense bulk MgB_2 under vacuum or ambient pressure conditions.[28] Starting from elemental powders, high dense massive MgB_2 has been obtained by using high pressure (up to 10 GPa) techniques only. These pressure levels (> 1 GPa) allow one to minimize the magnesium evaporation responsible for residual porosity. Nevertheless, the SPS technique makes it possible to synthesize bulk MgB_2 samples with density values higher than those obtained by means of conventional routes, such as Powder In Tube (PIT) methods or vacuum/ambient pressure sintering.[28] Furthermore, as will be shown in the next section, the SPS product shows superconducting properties comparable with those characteristic of dense samples obtained by high pressure methods.

Superconducting properties

Four SPS samples (identified as D, L, N, and Q) have been subjected to transport and magnetic measurements in order to evaluate their superconducting features.

Figure 9 shows the resistivity of the samples sintered under different operating conditions, in the temperature range 10-300 K. Table 5 gives the superconductive critical temperature measured resistivity ($T_{c,res}$) and magnetization ($T_{c,magn}$), the width of the superconductive transition measured by resistivity (ΔT_{res}) and magnetization (ΔT_{magn}), the resistivity at 40 K

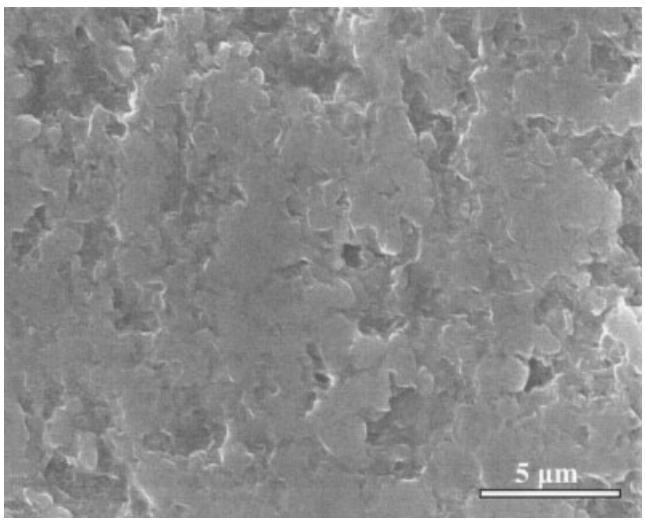

Figure 8. SEM micrograph of the SPS end-product (T_D = 800°C, P = 50 MPa, t_T = 10 min, t_D = 5 min).

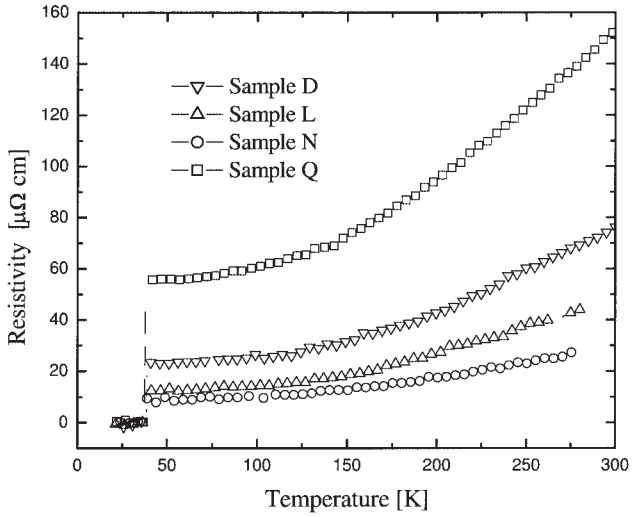

Figure 9. Resistivity of different SPS end-products as a function of temperature.

(ρ_{40K}), and the filed cooling magnetization at 5 K (M_{5K}). It is shown that the samples have a transition to the superconducting state between 38.7 K (sample L) and 37.4 K; the transition width is in the range from 0.2 K (sample N) to 0.4 K. The lowest absolute value of resistivity at room temperature is 30 $\mu\Omega$·cm and corresponds to sample N while the residual resistivity ratio (RRR) is about equal to 3, which is in good agreement with the results reported in the literature.[10,32] The resistivity before transition (40 K) shows a large variation in the samples since the value corresponding to sample Q is six times the value related to sample N. This difference can be due only to a different resistance of the intergrain connections.

The measurement of the DC magnetization at 1 Oe as a function of temperature was performed on bulk and powdered samples. The zero-field cooling (ZFC) and the field cooling (FC) magnetization at 1 Oe measured on bulk samples, normalized to the low-temperature value, are shown in Figure 10. Table 5 reports the critical temperature, measured as onset of the magnetic transition, and the width, determined as the interval between 90% and 10% of the magnetization jump. The transition temperature varies between 38.2 K and 38.4 K and the width is equal to 0.4-0.5 K. The large difference between the ZFC and FC curves indicates that, even in a very low field, there is a strong pinning of magnetic flux during the field cooling.[28,32] The magnetization at 1 Oe has been measured also on powdered samples in order to evaluate the absolute value with the approximation of the uniformly magnetized spheres.[33] The corresponding values at 5 K are reported in Table 5, where it is seen that the largest ones correspond to samples D and N.

Since the transition width has been related to the connection

Table 5. Resistive and Magnetic Data*

Sample ID	$T_{c,res}$ [K]	ΔT_{res} [K]	ρ_{40K} [$\mu\Omega \cdot$ cm]	$T_{c,magn}$ [K]	ΔT_{magn} [K]	M_{5K} [emu/cm]^3
D	38.4	0.3	24	38.2	0.4	−0.065
L	38.7	0.3	12.8	38.2	0.5	−0.058
N	38.2	0.2	9.2	38.4	0.4	−0.065
Q	37.4	0.4	56	38.2	0.5	−0.051

*Uncertainties on the measured values are equal to one unit of the last digit.

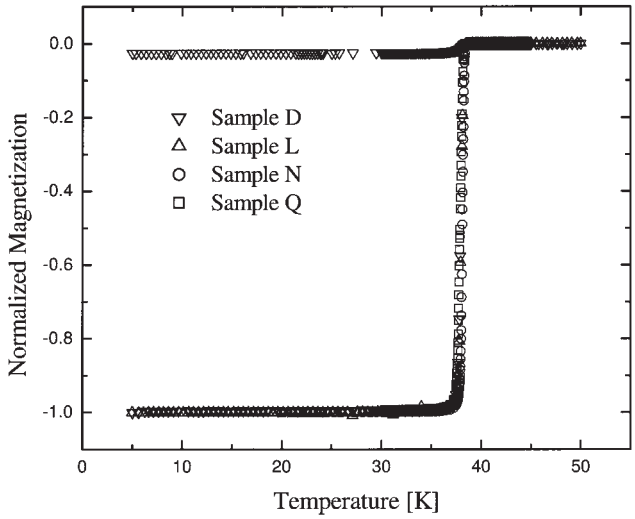

Figure 10. Normalized magnetization of different SPS end-products as a function of temperature.

among sample grains, it is possible to state that the obtained sample reveals a sharp transition from normal to superconducting state due to good grain connectivity. Moreover, it should be noted that the obtained superconducting transition width is comparable with higher density products obtained by means of other techniques.[10,34] In addition, the obtained normal state resistivity is found to be very close to that characteristic of denser samples.[28]

From the transport and magnetic properties given in Table 5, sample N has been chosen for further characterizations due to its superconducting properties. Figure 11 shows the hysteresis loop measured at 5 and 20 K, with applied field starting from zero to 50 kOe. The measurement has been performed on a powdered sample with particles of mean size 0.40 μm, measured by SEM.

The critical current density as a function of the applied field ($J_c(H)$) of sample N at 5 and 20 K has been determined by the

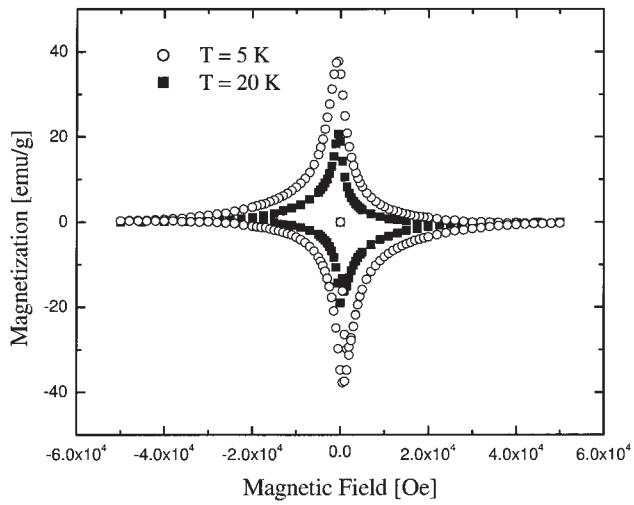

Figure 11. Magnetization of the SPS end-product as a function of magnetic field (T_D = 800°C, P = 50 MPa, t_T = 65 min, t_D = 5 min).

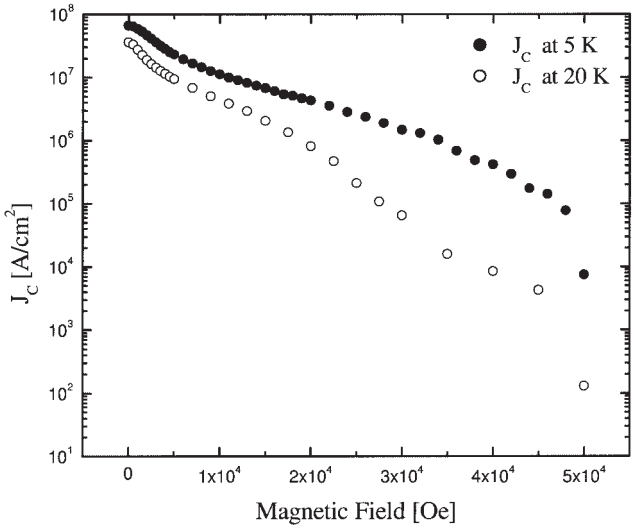

Figure 12. Critical current density of the SPS end-product as a function of magnetic field (T_D = 800°C, P = 50 MPa, t_T = 65 min, t_D = 5 min).

hysteresis loop using the Bean critical state model[35] and the equation for powder samples[36]:

$$J_c(H) = 3\Delta m_{total}(H)/(4V_{total}R_0) \quad (1)$$

where $\Delta m_{total}(H)$ is the difference between the values of the magnetic moment of the powder at a field value H, V_{total} is the total volume of the powder, and R_0 is the mean radius of the particles. The resulting J_c is shown in Figure 12. The obtained current density is actually the intragrain J_c, which is equal to the intergrain J_c because the current density is not limited by intergrain connections in MgB_2.[7] The obtained values are higher than those reported in the literature,[7,28,36] even when SPS is used for sintering purposes only.[19]

The improvement of transport and magnetic properties of SPS products is associated with the increase of the duration of the thermal treatment (particularly in sample N). Conversely, the synthesis with pressures higher than 50 MPa makes these properties worse, especially the transport ones. This is probably due to the formation of a phase with high resistance at the intergrain connections.

Conclusions

On the basis of the results described above, it can be concluded that the most significant and rapid sample shrinkage indicates that Mg melts and start to react with B to form the diboride phase. However, this fact is not a manifestation of the completeness of the MgB_2 formation, which, on the other hand, requires additional synthesis time in the SPS.

The superconducting properties of the obtained samples, measured both with transport and magnetic measurements, are comparable to or better than those corresponding to other MgB_2 preparation techniques. Thus, the superconductive properties of the bulk MgB_2 materials synthesized following the process proposed in this work are suitable for selected applications, such as magnetic levitation, magnetic screening, and fault current limiters. The sample prepared with the longest

thermal treatment (sample N) shows the best superconducting properties.

It should be finally noted that the proposed method to simultaneously synthesize and consolidate bulk MgB_2 superconductors from Mg and B elemental powders represents a particularly rapid preparation route as compared to the techniques available in the literature. This general consideration results to be even more specific when comparing the proposed protocol to previous ones that take advantage of the same SPS apparatuses.[18-20]

Literature Cited

1. Jones M, Marsh R. The preparation and structure of magnesium diboride, MgB_2. *J Am Ceramic Soc*. 1954;76:1434-1436.
2. Nagamatsu J, Nakagawa N, Muranaka T, Zenitani Y, Akimitsu J. Superconductivity at 39 K in magnesium diboride. *Nature.* 2001;410: 63-64.
3. Dai W, Feng QR, Gao ZX. Superconductivity in MgB_2. *Progress in Natural Science.* 2002;12:801-807.
4. Canfield PC, Bud'ko SL, Finnemore DK. An overview of the basic physical properties of MgB_2. *Physica C.* 2003;385:1-7.
5. Naito M, Ueda K. MgB_2 thin films for superconduction electronics. *Superconductors Science Technology.* 2004;17:R1-R18.
6. Scanlan RM, Malozemoff AP, Larbalestier DC. Superconducting materials for large scale applications. *Proceedings of the IEEE.* 2004;92: 1639-1654.
7. Buzea C, Yamashita T. Review of the superconducting properties of MgB_2. *Superconductor Science Technology.* 2001;14:R115-R146.
8. Rogado N, Hayward MA, Regan KA, Wang YY, Ong NP, Zandbergen HW, Rowell JM, Cava RJ. Low temperature synthesis of MgB_2. *J Appl Phys.* 2001;91:274-277.
9. Drozd VA, Gabovich AM, Gierlowski P, Pekala M, Szymczak H. Transport properties of bulk and thin film MgB_2 superconductors: effects of preparation conditions. *Physica C.* 2004;402:325-334.
10. Jung CU, Park MS, Kang WN, Kim MS, Kim KHP, Lee SY, Lee SI. Effect of sintering temperature under high pressure on the superconductivity of MgB_2. *Appl Phys Lett.* 2001;78:4157-4159.
11. Prikhna TA, Gawalek W, Savchuk YM, Surzhenko AB, Zeisberger M, Moshchil VE, Dub SN, Melnikov VS, Sergienko NV, Habisreuther T, Litzkendorf D, Abell S, Nagorny PA. High pressure synthesis and sintering of MgB_2. *IEEE Transactions on Appl Superconductivity.* 2003;13:3506-3509.
12. Gumbel A, Perner O, Eckert J, Fuchs G, Nenkov K, Muller KH, Schultz L. High density nanocrystalline MgB_2 bulk superconductors with improved pinning. *IEEE Transactions on Appl Superconductivity.* 2003;13:3064-3067.
13. Tampieri A, Celotti G, Sprio S, Caciuffo R, Rinaldi D. Study of the sintering behaviour of MgB_2 superconductor during hot-pressing. *Physica C.* 2004;400:97-104.
14. Giunchi G. High density MgB_2 obtained by reactive liquid infiltration. *Int J Modern Phys B.* 2003;17:453-460.
15. Agostino A, Bonometti E, Volpe P, Truccato M, Manfredotti C, Olivero P, Paolini C, Rinaudo G, Gozzelino L. Carbon influence in the synthesis of MgB_2 by a microwave method. *Int J Modern Phys B.* 2003;17:773-778.
16. Matsuzawa H, Tamaki H, Ohashi W, Kakimoto E, Dohke K, Atou T, Fukuoka K, Kikuchi M, Kawasaki M, Takano Y. Shock wave consolidated MgB_2 bulk samples. *Physica C.* 2004;412-414(Part 1):619-622.
17. Omori M. Sintering, consolidation, reaction and crystal growth by spark plasma system (SPS). *Mat Sci Eng.* 2000;A287:183-188.
18. Lee SY, Yoo SI, Kim YW, Hwang NM, Kim DY. Preparation of dense MgB_2 bulk superconductors by spark plasma sintering. *J Am Ceramic Soc.* 2003;86:1800-1802.
19. Shim SH, Shim KB, Yoon JW. Superconductivity characteristics of polycrystalline magnesium diboride ceramics fabricated by a Spark Plasma Sintering techniques. *J Am Ceramic Soc.* 2005;88:858-861.
20. Schmidt J, Schnelle W, Grin Y, Kniep R. Pulse plasma synthesis and chemical bonding in magnesium diboride. *Solid State Sciences.* 2003; 5:535-539.
21. Cao G, Locci AM, Orrù R. *Processo per la preparazione di un prodotto superconduttore a base di diboruro di magnesio, e prodotto ottenibile con tale processo*. Italian Patent No. FI2004A000208; 2004.
22. Cao G, Locci AM, Orrù R. *Process for the Preparation of a MgB_2-Based Superconducting Product, and Product Obtainable by This Process.* European Patent No. PCT/EP2005/052857; 2005.
23. Rowell JM. The widely variable resistivity of MgB_2 samples. *Superconductor Science Technology.* 2003;16:R17-R27.
24. Gedevanishvili S, Munir ZA. The synthesis of TiB_2-$TiAl_3$ composites by field-activated combustion. *Mat Sci Eng.* 1998;A246:81-85.
25. Chen C, Zhou ZJ, Li XG, Xu J, Wang YH, Wang YZ, Feng QR. Phase formation of polycrystalline MgB_2 using nanometer Mg powder. *Solid State Commun.* 2004;131:275-278.
26. Feng QR, Chen CP, Xu J, Kong LW, Chen X, Wang YZ, Zhang Y, Gao ZX. Study on the formation of MgB_2 phase. *Physica C.* 2004; 411:41-46.
27. Yan G, Feng Y, Fu BQ, Liu CF, Zhang PX, Wu XZ, Zhou L, Zhao Y, Pradhan AK. Effect of synthesis temperature on density and microstructure of MgB_2 superconductor at ambient pressure. *J Mat Sci.* 2004;39:4893-4898.
28. Takano Y, Takeya H, Fujii H, Kumakura H, Hatano T, Togano K. Superconducting properties of MgB_2 bulk materials prepared by high pressure synthesis. *Appl Phys Lett.* 2001;78:2914-2916.
29. Zlotnikov I, Gotman I, Gutmanas EY. Reactive processing of dense MgB_2 superconductor from Mg-2B powder blend. *Int J Self-Propagating High-Temperature Synthesis.* 2003;12:295-301.
30. Liu ZK, Schlom DG, Li Q, Xi XX. Thermodynamics of the Mg-B system: implication for the deposition of the MgB_2 thin films. *Appl Phys Lett.* 2001;78:3678-3680.
31. Fan ZY, Hinks DG, Newman N, Rowell JM. Experimental study of MgB_2 decomposition. *Appl Phys Lett.* 2001;79:87-89.
32. Indrakanti SS, Nesterenko VF, Maple MB, Frederick NA, Yuhasz WH, Li S. Hot isostatic pressing of bulk magnesium diboride: mechanical and superconducting properties. *Philosophical Magazine Lett.* 2001;81:849-857.
33. Zijlstra H. *Experimental Methods in Magnetism*, Vol. 2. Amsterdam: North-Holland; 1967.
34. Ren ZA, Che GC, Zhao ZX, Chen H, Dong C, Ni YM, Jia SL, Wen HH. Superconducting properties of MgB_2 prepared by high and ambient pressures. *Chinese Phys Lett.* 2001;18:589-591.
35. Bean CP. Magnetization of high-field superconductors. *Rev Mod Phys.* 1964;36:31-39.
36. Dhallé M, Toulemonde P, Beneduce C, Musolino N, Decroux M, Flukiger R. Transport and inductive critical current densities in superconducting MgB_2. *Physica C.* 2001;363:155-165.

Manuscript received Aug. 4, 2005, and revision received Feb. 20, 2006.